Random adsorption process of linear *k*-mers on square lattices under the Achlioptas process

Fuxing Chen,[1] Ping Fang,[1] Liangsheng Li,[2] Wen-Long You,[3] and Maoxin Liu[1,*]
[1]*School of Science, Beijing University of Posts and Telecommunications, Beijing 100876, China*
[2]*Science and Technology on Electromagnetic Scattering Laboratory, Beijing 100854, China*
[3]*College of Science, Nanjing University of Aeronautics and Astronautics, Nanjing 211106, China*

(Received 9 March 2022; accepted 26 May 2022; published 15 June 2022)

We study the explosive percolation with *k*-mer random sequential adsorption (RSA) process. We consider both the Achlioptas process (AP) and the inverse Achlioptas process (IAP), in which giant cluster formation is prohibited and accelerated, respectively. By employing finite-size scaling analysis, we confirm that the percolation transitions are continuous, and thus we calculate the percolation threshold and critical exponents. This allows us to determine the universality class of the *k*-mer explosive percolation transition. Interestingly, the numerical simulation suggests that the universality class of the explosive percolation transition with the AP alters when the *k*-mer size changes. In contrast, the universality class of the transition with the IAP is independent of *k*, but it differs from that of the RSA without the IAP.

DOI: 10.1103/PhysRevE.105.064116

I. INTRODUCTION

The random sequential adsorption (RSA) model, which describes the irreversible adsorption processes, plays an important role in statistical physics [1–3]. It has been widely applied to multiple scientific fields such as physics, chemistry, and biology, ranging from protein deposition kinetics [4], adsorption and desorption of human serum albumin on hydroxyapatite [5], adsorption of Brownian particles onto solid surfaces [6], nanoparticle deposition on heterogeneous surfaces [7], the kinetics adsorption of colloidal particles [8,9], to the parking model [10]. In the RSA model, shaped objects are randomly adsorbed on an initially empty substrate, with the restriction that they are not allowed to overlap with each other. In a lattice model, the deposited object can be represented by a straight line with k nearest sites (or bonds), known as the so-called *k*-mers [11,12].

In the RSA process of *k*-mers, when the concentration of the deposited *k*-mers reaches a certain critical value, a giant cluster with macroscopic scale arises, corresponding to the percolation threshold [13]. Due to its importance in critical phenomena, the criticality of the percolation of *k*-mers has been extensively studied from miscellaneous perspectives, including different lattice geometries (e.g., a square lattice [14–18], a triangular lattice [19–21], a honeycomb lattice [22], and a three-dimensional square lattice [23]), different *k*-mer shapes (e.g., the bendable *k*-mer object [24–28], the site-bond mixed *k*-mers [21,29], heteronuclear dimers [30], and monomer-polyatomic mixtures [16]), and extended *k*-mers RSA issues (e.g., the inverse adsorbed process of *k*-mers [31–34], and the anisotropic and isotropic adsorbed process of *k*-mers [35–40]). These studies show that percolation properties depend strongly on the lattice structure and the shape of deposited particles. The behavior of the percolation threshold is also affected by impurity particles [11,12,19,27,30,34,38–43]. Despite much variability, it has been well recognized that the percolation transitions of the above-mentioned kaleidoscopic models all belong to the random percolation universality class [11,12,15–17,21–26,31–35,41,43,44]. These results agree with the spirit of universality, in the sense that the universality class is independent of the microscopic details such as the shape of *k*-mers or the geometry of the lattice.

Recently, the so-called explosive percolation was introduced with the Achlioptas process (AP), in which a newly added edge with minimum cluster production is chosen from several random candidates during each step [45–47]. An immediate result is that the percolation transition is delayed yet it becomes sharper and more sudden. The explosive percolation transition was first considered to be discontinuous, but soon it was confirmed to remain continuous [48–54]. Despite the subtle continuity [55], one finds that the universality class of the explosive percolation is no longer the same as that of the random percolation [51,56–58]. This motivates us to consider the universality class of the explosive *k*-mer percolation. A natural question arises regarding whether the percolation of *k*-mer universality is robust and unrelated to the *k*-mer size k when the AP is introduced. We also note that an inverse Achlioptas process (IAP) has been considered in which the critical exponent is equal to the random percolation [59]. In the present article, the percolation of the AP and the IAP adsorption of linear *k*-mers on two-dimensional (2D) square lattices is investigated by using numerical simulations [60] and finite-size scaling analysis [61,62]. The numerical results of percolation thresholds are obtained as a function of the size of *k*-mers, which show similar decreasing behavior with the RSA process for the AP and the IAP. Interestingly, the increasing value of critical exponent β/ν reflects that the universality class is governed by the *k*-mer size for the AP,

*liumaoxin@bupt.edu.cn

while for the IAP the invariant exponents β/ν and ν indicate that the universality is irrespective of the k-mer size.

Our paper is organized as follows. The model for the k-mer AP and IAP and the simulation algorithm are given in Sec. II. The finite-size scaling of the percolation transition is introduced in Sec. III. In Sec. IV, the results of numerical simulation of the percolation threshold and critical exponents are presented. Finally, we present a summary and discussion in Sec. V.

II. MODEL

The linear k-mer object is defined as a linear array of k occupied sites on a lattice. The k-mer percolation model describes the dynamic process, in which the lattice is randomly filled with k-mers. With a large enough concentration of the deposited k-mers, a macroscopic scale of the k-mer cluster emerges. Conventionally, the model assumes the absence of overlap of the new incoming k-mers with the previously added ones. It leads to the jamming limit in the k-mer adsorption dynamics [63,64], which is reached when it is not possible to place any more k-mers before the lattice is fulfilled. Thus, it is possible that the jamming happens before it percolates if the value of k is large. In this work, however, we consider only small values of k, where the jamming effect is irrelevant.

We consider the deposition of the k-mer model incorporating the AP [45]. Starting from an empty lattice, two candidate k-mers are chosen uniformly at random at each discrete time step. Each k-mer may connect a certain number of clusters, and the picked k-mer is the one minimizing the product of the sizes of clusters linked by the k-mers. This competitive procedure, called the product rule, slows down considerably the emergence of the percolation cluster of k-mers. Thus, it is extremely abrupt when the so-called explosive percolation transition eventually happens. In the simulation, one of the two k-mers is deposited randomly but competitively on the lattice. To be more precise, the procedure for the product rule consists of five steps:

(i) Initially, two k-mers of length k are chosen from any available lattice sites at random.

(ii) The candidate k-mers are adjacent to a certain number of distinct clusters with sizes, respectively, denoted by the set $S_c = \{S_{c1}, S_{c2}, \ldots, S_{ci}\}$.

(iii) Next, we calculate the product of the candidate k-mer by $\prod_{ci} S_{ci}$.

(iv) The candidate k-mer with a smaller product is kept as new occupied sites on the lattice, while another one is eliminated.

(v) Repeat the previous steps until jamming happens.

For comparison, we might as well introduce the IAP [59] as well, which only needs to retain the k-mers with a large product instead of the small ones in step (iv) of the above procedure. Contrary to the AP, the IAP will reward the growth of large clusters.

In Fig. 1, we present a schematic description of the product rule of the AP. At a given instance, the lattice has deposited a few clusters, namely a cluster of 12 sites and four clusters of 3 sites. Two candidate k-mers of length $k = 3$, i.e., k_1 and k_2, are selected randomly. The k_2 k-mers will be kept because the product of the cluster sizes that connects ($3 \times 3 \times 3 = 27$) is smaller than that of the k_1 k-mers ($12 \times 3 = 36$). For the IAP, the winner of the competition should be k_1 k-mers.

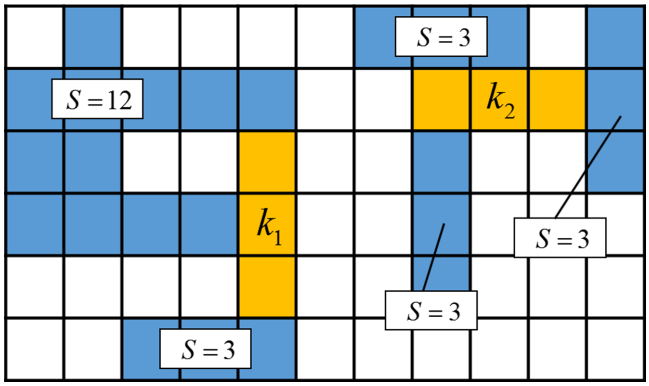

FIG. 1. For $k = 3$, the products of two candidate k-mers (labeled by k_1 and k_2) are calculated. The product of k_1 is $12 \times 3 = 36$ and the product of k_2 is $3 \times 3 \times 3 = 27$. According to the product rule, the k-mers k_2 should be retained finally for the AP, while for the IAP the k-mers k_1 should be kept.

To investigate the k-mers percolation of the AP and the IAP, we trace the clusters in Monte Carlo simulation, especially for the largest cluster and the second largest cluster. We can perform the task by using the Union-Find algorithm of Ziff and Newman [60]. The second cluster will probably be annexed by the rest of the clusters in some steps; to traverse the lattice for the new second cluster is a compromise.

In the later period, straightforward attempts of mass-election for candidate k-mers are time-consuming due to the scarcity of viable lattice sites. This problem can be solved by generating four arrays of viable sites [65] as a starting point, and a k-mer can be placed in the corresponding orientation. Randomly, the candidate k-mers are selected from the updating arrays at each step until all elements are exhausted.

In our simulations, a set of 2×10^6 independent random samples are prepared for small k-mers ($1 \leqslant k \leqslant 10$). In addition, we consider the substrate being represented by a 2D square lattice of $N = L \times L$ sites with periodic boundary conditions. For each length k of k-mers, the finite-size effect is examined on lattices of linear size $L = 512, 1024, 2048, 4096$ for both AP and IAP.

III. FINITE-SIZE SCALING

The percolation transition of Achlioptas-type processes has been proved as a second-order phase transition [48,51], and the k-mer explosive percolation is expected to be the same. As is known in the percolation theory, the probability of the percolation increases with the concentration p. For continuous percolation systems on a finite lattice, the scaling theory allows us to estimate the dependence of the percolation cluster size $S(k; p, L)$ on the linear lattice size L. Near the transition point p_c of the percolation, a finite-size scaling form of reduced sizes

$$s(k; p, L) \equiv \frac{S(k; p, L)}{L \times L} \tag{1}$$

is anticipated as [61,62]

$$s(k;p,L) = L^{-\beta/\nu}\tilde{s}(k;tL^{1/\nu}), \tag{2}$$

which is supposed to be valid in the asymptotic critical region of $L \gg k$ and $\|t\| \ll 1$. Here $t = (p - p_c)/p_c$, and the correlation-length exponent ν describes the power-law divergence of the correlation length ξ at the critical threshold p_c, i.e., $\xi = \xi_0\|t\|^{-\nu}$. For the largest cluster of k-mers on the lattice, the scaling form in Eq. (2) is rewritten as

$$s_1(k;p,L) = L^{-\beta/\nu}\tilde{s}_1(k;tL^{1/\nu}). \tag{3}$$

Similarly, for the second largest cluster of k-mers, it yields

$$s_2(k;p,L) = L^{-\beta/\nu}\tilde{s}_2(k;tL^{1/\nu}). \tag{4}$$

In the thermodynamic limit $L \to \infty$, the order parameter s_1 abruptly increases to a finite value at $p = p_c$. For $p > p_c$, $s_1 \propto t^{\beta}$.

By observing Eqs. (3) and (4), a finite-size scaling form of the ratio parameter U could be defined:

$$U(k;tL^{1/\nu}) \equiv s_2/s_1 = \tilde{s}_2(k;tL^{1/\nu})/\tilde{s}_1(k;tL^{1/\nu}). \tag{5}$$

In addition, by taking the logarithm of Eq. (3), we can have the following relationship:

$$\ln s_1(k;p,L) = -(\beta/\nu)\ln L + \ln\tilde{s}_1(k;tL^{1/\nu}). \tag{6}$$

At the critical point $p = p_c$, the ratio parameter U reads

$$U(k;tL^{1/\nu}) = (s_2/s_1)|_{p=p_c} = U(k;0), \tag{7}$$

which is independent of the lattice size L. Therefore, there is a fixed point $U(k;0)$ for curves of U versus L at the critical threshold. In the actual numerical simulations, the asymptotic behavior of the cross point is predictable due to the finite-size correction term. Thus, a larger lattice size L is better.

Moreover, according to Eq. (5), for a given k-mer of length k, in the range of $p \to p_c$ and $L \gg k$, using the scaling variable $tL_{1/\nu}$ with a properly chosen exponent ν, different curves of $U(k;tL^{1/\nu})$ with various lattice sizes L collapse onto the size-independent scaling function. At the critical point $p = p_c$, according to Eq. (6), we have

$$\ln s_1(k;p,L) = -(\beta/\nu)\ln L + \ln\tilde{s}_1(k;0), \tag{8}$$

where $\ln\tilde{s}_1(k;0)$ is a constant. This indicates the linear relationship between $\ln s_1(k;p,L)$ and $\ln L$. Thus, the critical point p_c and the critical exponent β/ν can be determined.

IV. NUMERICAL SIMULATION RESULTS

A. Percolation threshold

In the preceding section, the finite-size scaling of percolation was introduced. To proceed, as an illustrative example, we present the detailed numerical results of the percolation threshold and critical exponents through finite-size scaling for the k-mers with $k = 6$ in the given AP. In Fig. 2(a), for lattice sizes L from 512 to 1024, we plot the reduced sizes of the two largest clusters s_1 and s_2 as a function of the reduced k-mer numbers $p = kN_p/N$, where N_p is the number of deposited k-mers on the lattice. The order parameter s_1 becomes macroscopic for $p > p_c$. As the lattice size increases, the phase-transition process becomes abrupt and marked.

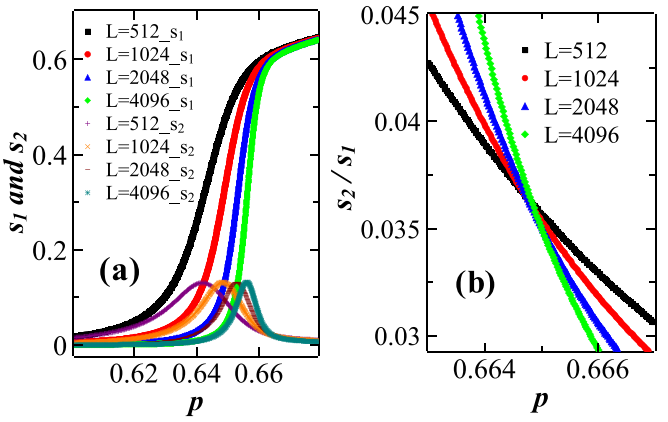

FIG. 2. (a) The reduced sizes of the largest (second largest) cluster s_1 (s_2) and (b) the ratio parameter U as a function of the concentration p with different lattice sizes for the AP with $k = 6$.

As we have discussed in Sec. III, the critical point can be determined by two methods. According to Eq. (7), for $k = 6$, an observed fixed point $U(k|_{=6};tL_{1/\nu}|_{=0})$ is independent of the system size at the phase-transition point. As is shown in Fig. 2(b), the curves of the ratio s_2/s_1 are shown as a function of the concentration p. For different L, the curves cross each other at $p = 0.664\,95 \pm 0.000\,15$, which allows for the determination of the percolation threshold $p_{c1} = 0.664\,95(15)$.

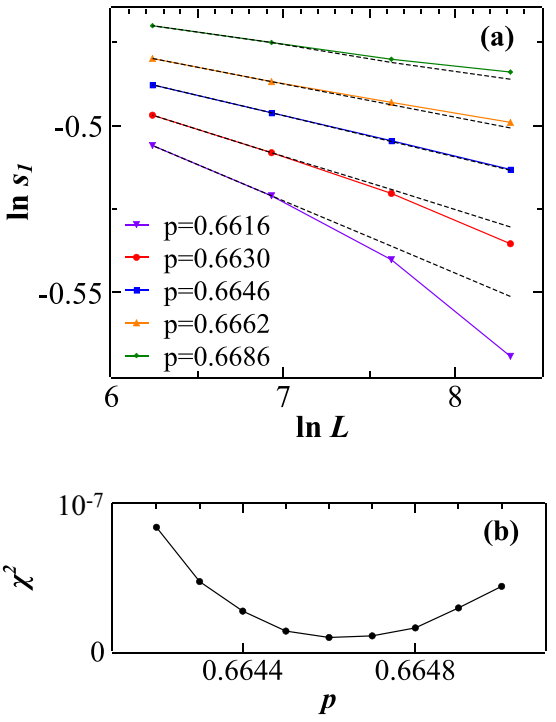

FIG. 3. (a) $\ln s_1$ vs $\ln L$ for different concentrations p with $k = 6$ in the AP. Here $L = 512$, 1024, 2048, and 4096. The black dotted lines are linear rules to guide the eyes. When $p \leqslant 0.6630$ and $p \geqslant 0.6662$, the curves show the obvious deviation from the linearity. (b) The residual sum χ^2 of the least-squares method for curves $0.6642 \leqslant p \leqslant 0.6650$. At $p = 0.6646$, the curve with the smallest χ^2 is closest to the linearity, implying the critical threshold $p_{c2} = 0.6646(4)$ and critical exponent $\beta/\nu = 0.123(9)$.

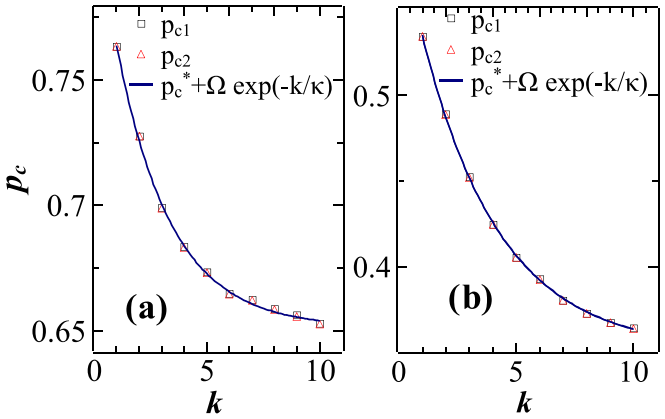

FIG. 4. For small-size k-mer percolation for (a) the AP and (b) the IAP, $1 \leqslant k \leqslant 10$, the critical thresholds p_{c1} and p_{c2} decrease with k. We can use the exponentially decreasing function in Eq. (9) to fit the monotonic behavior of the critical threshold. The fitting parameters for the AP are $p_c^* = 0.6515(3)$, $\Omega = 0.169\,91(17)$, and $\kappa = 2.413(4)$. The fitting parameters for the IAP are $p_c^* = 0.3508(3)$, $\Omega = 0.2495(1)$, and $\kappa = 3.32(1)$.

In addition, according to the theoretical prediction in Eq. (8), for the exact linear relationship between $\ln s_1$ and $\ln L$, the corresponding concentration p yields the critical threshold. As is shown in Fig. 3(a), the colored solid lines denote $\ln s_1$ as a function of $\ln L$ for different values of p, while the black dotted lines are the corresponding linear guide to the eye. The slopes of curves change with p from negative to positive at $p = 0.6616$, 0.6630, 0.6646, 0.6662, and 0.6686. When $p \leqslant 0.6630$ and $p \geqslant 0.6662$, the curves show obvious deviations from the linearity, The curve is closest to being linear around 0.6642–0.6650. As is shown in Fig. 3(b), in order to determine the most linear curve, we plot the residual sum χ^2 of the least-squares method for different p values in this range. At $p = 0.6646$, the curve with the smallest χ^2 is closest to the linearity. Thus, we obtain the critical point $p_{c2} = 0.6646(4)$ and critical exponent $\beta/\nu = 0.123(9)$.

The procedure for obtaining p_{c1} and p_{c2} can be repeated for k ranging between 1 and 10. The numerical results are shown in Fig. 4 and Table I. It is evident that the difference between p_{c1} and p_{c2} is negligible. For small-size k-mers ($1 \leqslant k \leqslant 10$), the percolation threshold as a function of k shows an exponential decrease, which resembles the RSA process on the square lattice [15]. We can use the following ansatz to fit the explosive percolation threshold:

$$p_c(k) = p_c^* + \Omega \exp\left(-\frac{k}{\kappa}\right). \tag{9}$$

The obtained fitting parameters of k-mers for the AP are $p_c^* = 0.6515(3)$, $\Omega = 0.169\,91(17)$, and $\kappa = 2.413(4)$. However, these fitting parameters are different from those in the RSA process, namely, $p_c^* = 0.456(31)$, $\Omega = 0.196(5)$, and $\kappa = 2.92(20)$ (see our calculation in the Table I), which are almost equal to the values in Ref. [15]. The difference of p_c^* can be well understood because the AP will delay the percolation. The parameters Ω and κ characterize the extent to which the length of k-mers affects the percolation threshold. This indicates that the sensitivity of the percolation threshold of the AP to the k-mer size is different from that in the RSA process. Similarly, we can obtain the percolation thresholds p_{c1} and p_{c2} of the IAP, which are shown in Fig. 4 and Table I. The fitting parameters $p_c^* = 0.3508(3)$, $\Omega = 0.2495(1)$, and $\kappa = 3.32(1)$ according to Eq. (9). With the values of the critical points in hand, we can discuss finite-size effects. An effective critical point $p_c(L)$ can be defined as the peak position of the second largest cluster sizes (s_2) with a certain system size L. We expect a power-law relation between $p_c(L)$ and p_c in the thermodynamic limit:

$$|p_c - p_c(L)| = \xi L^{-\theta}, \tag{10}$$

where ξ is a universal constant and θ is a critical exponent. This relation can be rewritten as

$$\ln|p_c - p_c(L)| = \ln\xi - \theta \ln(L), \tag{11}$$

showing a linearity between $\ln(L)$ and $\ln|p_c - p_c(L)|$. In Fig. 5, we take the $k = 6$ case for an example to show the validity of Eq. (11).

B. Critical exponents and universality class

In this section, for the k-mer explosive percolation of the AP, critical exponents β/ν and ν are calculated, which significantly determine the universality class. Without a loss of generality, the case choosing $k = 6$ as an example is presented. In Fig. 3, the linear relationship between $\ln s_1$ and

TABLE I. For the AP, IAP, and RSA, the critical threshold p_c and exponents β/ν, ν of different k values are shown.

Rule	AP				IAP				RSA		
k	p_{c1}	p_{c2}	β/ν	ν	p_{c1}	p_{c2}	β/ν	ν	p_c	β/ν	ν
1	0.76337(8)	0.7633(6)	0.0100(8)	2.42(6)	0.5349(2)	0.53476(5)	0.111(4)	1.40(3)	0.59274(3)	0.106(4)	1.33(1)
2	0.72776(10)	0.7276(6)	0.0106(9)	2.40(6)	0.4892(3)	0.48898(5)	0.112(3)	1.41(3)	0.59191(3)	0.107(3)	1.34(2)
3	0.69929(11)	0.6990(13)	0.0113(5)	2.40(4)	0.4523(2)	0.45220(4)	0.110(3)	1.39(3)	0.52792(4)	0.106(4)	1.33(2)
4	0.68351(11)	0.6833(8)	0.0116(6)	2.41(5)	0.4247(2)	0.42455(5)	0.111(3)	1.39(2)	0.50496(5)	0.106(5)	1.34(2)
5	0.67350(18)	0.6733(7)	0.0117(10)	2.42(4)	0.4053(2)	0.40519(7)	0.110(5)	1.39(3)	0.49000(5)	0.105(4)	1.33(2)
6	0.66495(15)	0.6646(4)	0.0123(9)	2.36(6)	0.3925(2)	0.39242(5)	0.109(3)	1.38(3)	0.48021(5)	0.107(4)	1.34(2)
7	0.66247(25)	0.6621(6)	0.0128(9)	2.38(6)	0.3802(2)	0.38009(5)	0.109(3)	1.37(3)	0.47388(5)	0.106(4)	1.34(2)
8	0.65894(14)	0.6585(5)	0.0129(12)	2.38(6)	0.3725(2)	0.37238(5)	0.110(3)	1.38(2)	0.46971(4)	0.106(3)	1.33(2)
9	0.65627(10)	0.6558(7)	0.0133(13)	2.36(6)	0.3670(2)	0.36694(5)	0.109(3)	1.37(3)	0.46697(4)	0.107(3)	1.33(3)
10	0.65311(13)	0.6526(7)	0.0133(13)	2.38(6)	0.3638(2)	0.36369(5)	0.109(3)	1.38(3)	0.46523(4)	0.108(3)	1.32(2)

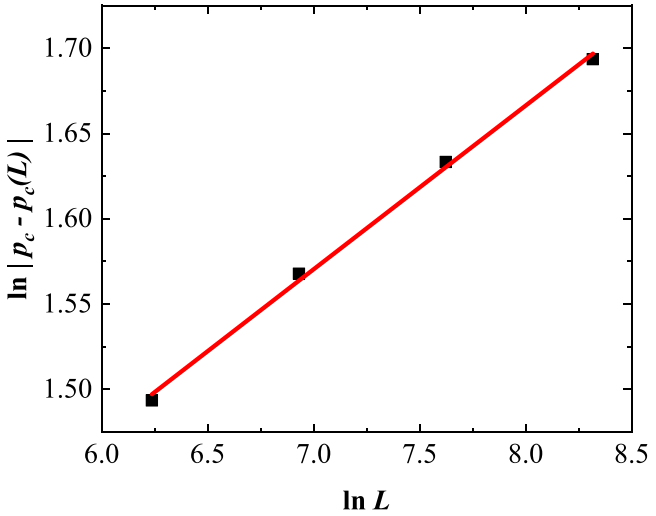

FIG. 5. $\ln|p_c - p_c(L)|$ vs $\ln L$ for $k = 6$, where $L = 512,\ 1024,\ 2048$, and 4096.

$\ln L$ is identified at $p_{c2} = 0.6646(4)$, and correspondingly the critical exponent $\beta/\nu = 0.123(9)$ is retrieved from the slope. According to the finite-size scaling theory in Eq. (5), using the obtained value of the critical point $p_{c1} = 0.664\,95(15)$ and the properly chosen value of the correlation-length exponent $\nu = 2.36(6)$, the curves U of different lattice sizes collapse together; see Fig. 6.

Accordingly, the scaling exponents β/ν and ν are numerically calculated for the k-mer explosive percolation with $1 \leqslant k \leqslant 10$, and they are listed in Table I. As is shown in Fig. 7, we plot the extracted critical exponent ν versus k. For $k \leqslant 10$, the obtained ν is almost unchanging within the error bar. Furthermore, Fig. 8 shows β/ν with respect to k. Nevertheless, one sees that β/ν increases monotonically with k. It is well known that systems belong to the same universality class when critical exponents and scaling functions are the same. It is anticipated that the percolation transition of the k-mer RSA process, which is independent of k, belongs to the same

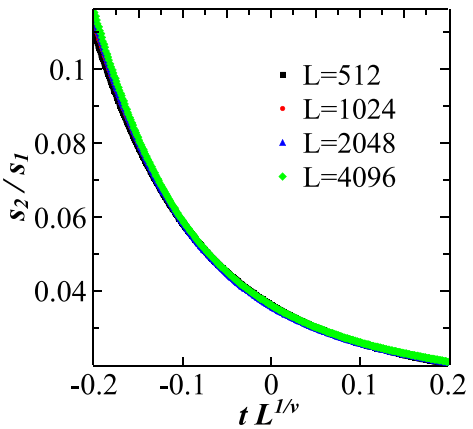

FIG. 6. The scaling function $U \equiv s_2/s_1$ with respect to the variable $tL^{1/\nu}$ with $t = (p - p_c)/p_c$. When $\nu = 2.36$ and $p_c = 0.664\,95$ are chosen, curves of different lattice sizes collapse together near $tL^{1/\nu} = 0$.

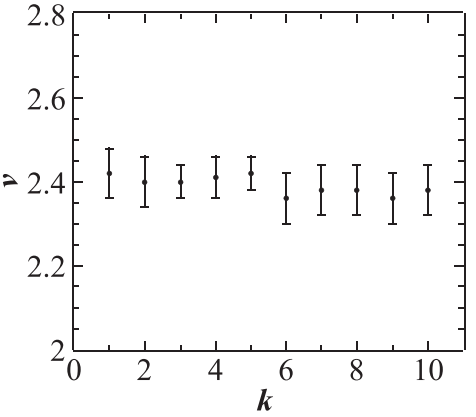

FIG. 7. For k-mer AP percolation, the critical exponent ν with respect to k in the range of $1 \leqslant k \leqslant 10$.

universality class with the random percolation. However, for the k-mer explosive percolation model, the exponent β/ν is different for each k, suggesting that it is in different universality classes. The fact that critical exponent β/ν is model parameter k-dependent demonstrates the nonuniversality of percolation phenomena for the AP of k-mers.

Similarly, the critical exponents for the IAP can be retrieved. The correlation-length exponents ν and β/ν versus k are plotted in Figs. 9 and 10, respectively. One readily finds that they almost remain constant, i.e., $\nu \approx 1.39(3)$ and $\beta/\nu \approx 0.110(3)$, as is shown in Table I. The feature that the universality behavior of the IAP is not related to the k-mer size is similar to that of the RSA process. It is known that the RSA process belongs to the random percolation universality class with critical exponents $\beta/\nu = 5/48$ and $\nu = 4/3$. However, the exponents of the IAP are subtly different.

V. DISCUSSION AND SUMMARY

In the present work, we study k-mer percolation ($1 \leqslant k \leqslant 10$) with both the AP and the IAP on two-dimensional square lattices. The percolation thresholds and critical exponents are

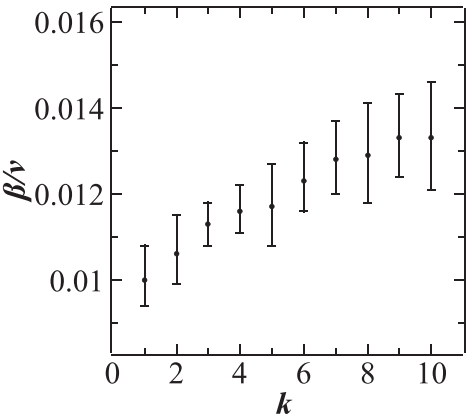

FIG. 8. For k-mer AP percolation, in the range of $1 \leqslant k \leqslant 10$, the critical exponent β/ν is obviously increasing with k. This suggests that the k-mer explosive percolation for each k belongs to different universality classes.

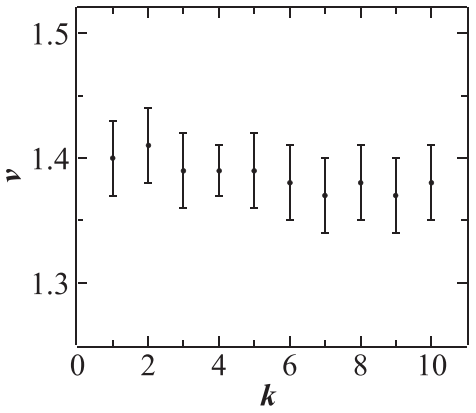

FIG. 9. The critical exponent ν for k-mer IAP percolation, in the range of $1 \leqslant k \leqslant 10$.

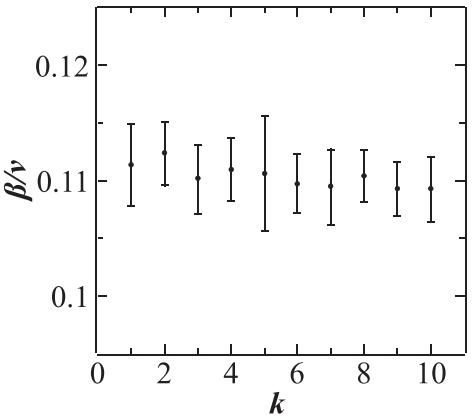

FIG. 10. The critical exponent β/ν for k-mer IAP percolation in the range of $1 \leqslant k \leqslant 10$.

calculated using Monte Carlo simulation with finite-size scaling analysis. We find that, with increasing k, the thresholds of the explosive k-mer percolation decrease, which agrees well with the ansatz in Eq. (9). For the AP, the correlation-length critical exponent ν is independent of k, while the order-parameter critical exponent β/ν increases with increasing k. To this end, we find an interesting phenomenon in that the universality class alters with the size of the microscopic component of the system. It has been recognized that a decrease of the critical exponent β corresponds to an increasing level of the competition [50]. Thus, it could suggest that the competition of the AP is depressed when k becomes larger. For the IAP, both the critical exponents ν and β/ν seem independent of k. The k-mers percolations with IAP belong to the same universality class for different values of k. We note that, in Ref. [59], an IAP independent critical exponent of τ is reported. However, in our study the exponent ν is different with and without the IAP. Thus, a comprehensive study is more likely to conclude that the percolation with and without IAP belongs to different universality classes. We also notice that a sufficiently large value of k could make a difference. For example, Eq. (9) breaks when k is sufficiently large [18,65]. Therefore, further study on the universality class of the k-mer explosive percolation should be interesting.

ACKNOWLEDGMENTS

This work is supported by the Fundamental Research Funds for the Central Universities (under Contracts No. 2021XD-A10 and No. 2020RC13) and the Natural Science Foundation of China (NSFC) (No. 12005024 and No. 12174194). W.-L.Y. kindly acknowledges support from the startup fund of Nanjing University of Aeronautics and Astronautics under Grant No. 1008-YAH20006, Top-notch Academic Programs Project of Jiangsu Higher Education Institutions (TAPP), and basic institute research under Grant No. 190101.

[1] P. Schaaf and J. Talbot, Kinetics of Random Sequential Adsorption, Phys. Rev. Lett. **62**, 175 (1989).
[2] J. W. Evans, Random and cooperative sequential adsorption, Rev. Mod. Phys. **65**, 1281 (1993).
[3] J. Talbot, G. Tarjus, P. Van Tassel, and P. Viot, From car parking to protein adsorption: An overview of sequential adsorption processes, Colloids Surf. A **165**, 287 (2000).
[4] J. J. Ramsden, Concentration Scaling of Protein Deposition Kinetics, Phys. Rev. Lett. **71**, 295 (1993).
[5] M. Mura-Galelli, J. Voegel, S. Behr, E. Bres, and P. Schaaf, Adsorption/desorption of human serum albumin on hydroxyapatite: A critical analysis of the langmuir model, Proc. Natl. Acad. Sci. USA **88**, 5557 (1991).
[6] B. Senger, J.-C. Voegel, P. Schaaf, A. Johner, A. Schmitt, and J. Talbot, Properties of jamming configurations built up by the adsorption of Brownian particles onto solid surfaces, Phys. Rev. A **44**, 6926 (1991).
[7] M. Sadowska, M. Cieśla, and Z. Adamczyk, Nanoparticle deposition on heterogeneous surfaces: Random sequential adsorption modeling and experiments, Colloids Surf. A **617**, 126296 (2021).
[8] P. Wojtaszczyk and J. B. Avalos, Influence of Hydrodynamic Interactions on the Kinetics of Colloidal Particles' Adsorption, Phys. Rev. Lett. **80**, 754 (1998).
[9] B. Senger, J.-C. Voegel, and P. Schaaf, Irreversible adsorption of colloidal particles on solid substrates, Colloids Surf. A **165**, 255 (2000).
[10] J. Talbot, G. Tarjus, and P. Viot, Sluggish kinetics in the parking lot model, J. Phys. A **32**, 2997 (1999).
[11] P. M. Centres and A. J. Ramirez-Pastor, Percolation and jamming in random sequential adsorption of linear k-mers on square lattices with the presence of impurities, J. Stat. Mech. (2015) P10011.
[12] V. Cornette, A. Ramirez-Pastor, and F. Nieto, Percolation of polyatomic species on site diluted lattices, Phys. Lett. A **353**, 452 (2006).
[13] R. M. Ziff, Spanning Probability in 2D Percolation, Phys. Rev. Lett. **69**, 2670 (1992).

[14] V. Cornette, A. Ramirez-Pastor, and F. Nieto, Dependence of the percolation threshold on the size of the percolating species, Physica A **327**, 71 (2003), Proceedings of the XIIIth Conference on Nonequilibrium Statistical Mechanics and Nonlinear Physics.

[15] V. Cornette, A. Ramirez-Pastor, and F. Nieto, Percolation of polyatomic species on a square lattice, Eur. Phys. J. B **36**, 391 (2003).

[16] M. Dolz, F. Nieto, and A. Ramirez-Pastor, Percolation processes in monomer-polyatomic mixtures, Physica A **374**, 239 (2007).

[17] D. Matoz-Fernandez, D. Linares, and A. Ramirez-Pastor, Nonmonotonic size dependence of the critical concentration in 2d percolation of straight rigid rods under equilibrium conditions, Eur. Phys. J. B **85**, 296 (2012).

[18] G. Kondrat, Z. Koza, and P. Brzeski, Jammed systems of oriented needles always percolate on square lattices, Phys. Rev. E **96**, 022154 (2017).

[19] G. Kondrat, The study of percolation with the presence of impurities, J. Chem. Phys. **122**, 184718 (2005).

[20] E. J. Perino, D. A. Matoz-Fernandez, P. M. Pasinetti, and A. J. Ramirez-Pastor, Jamming and percolation in random sequential adsorption of straight rigid rods on a two-dimensional triangular lattice, J. Stat. Mech. (2017) 073206.

[21] M. Quintana, I. Kornhauser, R. López, A. Ramirez-Pastor, and G. Zgrablich, Monte Carlo simulation of the percolation process caused by the random sequential adsorption of k-mers on heterogeneous triangular lattices, Physica A **361**, 195 (2006).

[22] G. A. Iglesias Panuska, P. M. Centres, and A. J. Ramirez-Pastor, Jamming and percolation of linear k-mers on honeycomb lattices, Phys. Rev. E **102**, 032123 (2020).

[23] G. D. Garcia, F. O. Sanchez-Varretti, P. M. Centres, and A. J. Ramirez-Pastor, Percolation of polyatomic species on a simple cubic lattice, Eur. Phys. J. B **86**, 403 (2013).

[24] G. Kondrat, Impact of composition of extended objects on percolation on a lattice, Phys. Rev. E **78**, 011101 (2008).

[25] W. Lebrecht, E. E. Vogel, J. F. Valdés, A. J. Ramirez-Pastor, P. M. Centres, M. I. González, and F. D. Nieto, Site trimer percolation on square lattices, Phys. Rev. E **92**, 012129 (2015).

[26] N. De La Cruz Félix, P. M. Centres, and A. J. Ramirez-Pastor, Irreversible bilayer adsorption of straight semirigid rods on two-dimensional square lattices: Jamming and percolation properties, Phys. Rev. E **102**, 012153 (2020).

[27] I. Lončarević, L. Budinski-Petković, D. Dujak, A. Karač, Z. M. Jakšić, and S. B. Vrhovac, The study of percolation with the presence of extended impurities, J. Stat. Mech. (2017) 093202.

[28] G. Kondrat, Influence of temperature on percolation in a simple model of flexible chains adsorption, J. Chem. Phys. **117**, 6662 (2002).

[29] M. Dolz, F. Nieto, and A. J. Ramirez-Pastor, Site-bond percolation of polyatomic species, Phys. Rev. E **72**, 066129 (2005).

[30] M. C. Gimenez and A. J. Ramirez-Pastor, Percolation of heteronuclear dimers irreversibly deposited on square lattices, Phys. Rev. E **94**, 032129 (2016).

[31] L. S. Ramirez, P. M. Centres, and A. J. Ramirez-Pastor, Inverse percolation by removing straight rigid rods from square lattices, J. Stat. Mech. (2015) P09003.

[32] L. S. Ramirez, P. M. Centres, and A. J. Ramirez-Pastor, Inverse percolation by removing straight rigid rods from triangular lattices, J. Stat. Mech. (2017) 113204.

[33] L. S. Ramirez, P. M. Centres, and A. J. Ramirez-Pastor, Standard and inverse bond percolation of straight rigid rods on square lattices, Phys. Rev. E **97**, 042113 (2018).

[34] L. S. Ramirez, P. M. Centres, and A. J. Ramirez-Pastor, Inverse percolation by removing straight rigid rods from square lattices in the presence of impurities, J. Stat. Mech. (2019) 033207.

[35] Y. Y. Tarasevich, N. I. Lebovka, and V. V. Laptev, Percolation of linear k-mers on a square lattice: From isotropic through partially ordered to completely aligned states, Phys. Rev. E **86**, 061116 (2012).

[36] L. S. Ramirez, P. M. Pasinetti, W. Lebrecht, and A. J. Ramirez-Pastor, Standard and inverse site percolation of straight rigid rods on triangular lattices: Isotropic and perfectly oriented deposition and removal, Phys. Rev. E **104**, 014101 (2021).

[37] A. L. R. Bug, S. A. Safran, and I. Webman, Continuum Percolation of Rods, Phys. Rev. Lett. **54**, 1412 (1985).

[38] Y. Y. Tarasevich, V. V. Laptev, A. S. Burmistrov, and T. S. Shinyaeva, Influence of anisotropy on percolation and jamming of linear k-mers on square lattice with defects, J. Phys.: Conf. Ser. **633**, 012064 (2015).

[39] Y. Y. Tarasevich, A. S. Burmistrov, T. S. Shinyaeva, V. V. Laptev, N. V. Vygornitskii, and N. I. Lebovka, Percolation and jamming of linear k-mers on a square lattice with defects: Effect of anisotropy, Phys. Rev. E **92**, 062142 (2015).

[40] I. Lončarević, L. Budinski-Petković, D. Dujak, A. Karač, Z. M. Jakšić, and S. B. Vrhovac, Percolation in irreversible deposition on a triangular lattice: Effects of anisotropy, J. Stat. Mech. (2020) 033211.

[41] V. Cornette, A. J. Ramirez-Pastor, and F. Nieto, Percolation of polyatomic species with the presence of impurities, J. Chem. Phys. **125**, 204702 (2006).

[42] Y. Y. Tarasevich, V. V. Laptev, N. V. Vygornitskii, and N. I. Lebovka, Impact of defects on percolation in random sequential adsorption of linear k-mers on square lattices, Phys. Rev. E **91**, 012109 (2015).

[43] N. I. Lebovka, Y. Y. Tarasevich, D. O. Dubinin, V. V. Laptev, and N. V. Vygornitskii, Jamming and percolation in generalized models of random sequential adsorption of linear k-mers on a square lattice, Phys. Rev. E **92**, 062116 (2015).

[44] P. Longone, P. M. Centres, and A. J. Ramirez-Pastor, Percolation of aligned rigid rods on two-dimensional triangular lattices, Phys. Rev. E **100**, 052104 (2019).

[45] D. Achlioptas, R. M. D'Souza, and J. Spencer, Explosive percolation in random networks, Science **323**, 1453 (2009).

[46] S. Boccaletti, J. Almendral, S. Guan, I. Leyva, Z. Liu, I. Sendiña-Nadal, Z. Wang, and Y. Zou, Explosive transitions in complex networks' structure and dynamics: Percolation and synchronization, Phys. Rep. **660**, 1 (2016).

[47] Y. Kang and Y. S. Cho, Scaling behavior of information entropy in explosive percolation transitions, Phys. Rev. E **104**, 014310 (2021).

[48] R. A. da Costa, S. N. Dorogovtsev, A. V. Goltsev, and J. F. F. Mendes, Explosive Percolation Transition is Actually Continuous, Phys. Rev. Lett. **105**, 255701 (2010).

[49] R. A. da Costa, S. N. Dorogovtsev, A. V. Goltsev, and J. F. F. Mendes, Critical exponents of the explosive percolation transition, Phys. Rev. E **89**, 042148 (2014).

[50] J. Nagler, A. Levina, and M. Timme, Impact of single links in competitive percolation, Nat. Phys. **7**, 265 (2011).

[51] P. Grassberger, C. Christensen, G. Bizhani, S.-W. Son, and M. Paczuski, Explosive Percolation is Continuous, but with Unusual Finite Size Behavior, Phys. Rev. Lett. **106**, 225701 (2011).

[52] H. K. Lee, B. J. Kim, and H. Park, Continuity of the explosive percolation transition, Phys. Rev. E **84**, 020101(R) (2011).

[53] S. Fortunato and F. Radicchi, Explosive percolation in graphs, J. Phys. Conf. Ser. **297**, 012009 (2011).

[54] O. Riordan and L. Warnke, Explosive percolation is continuous, Science **333**, 322 (2011).

[55] J. Nagler, T. Tiessen, and H. W. Gutch, Continuous Percolation with Discontinuities, Phys. Rev. X **2**, 031009 (2012).

[56] R. M. Ziff, Explosive Growth in Biased Dynamic Percolation on Two-Dimensional Regular Lattice Networks, Phys. Rev. Lett. **103**, 045701 (2009).

[57] N. Bastas, K. Kosmidis, and P. Argyrakis, Explosive site percolation and finite-size hysteresis, Phys. Rev. E **84**, 066112 (2011).

[58] J. Fan, M. Liu, L. Li, and X. Chen, Continuous percolation phase transitions of random networks under a generalized Achlioptas process, Phys. Rev. E **85**, 061110 (2012).

[59] R. A. da Costa, S. N. Dorogovtsev, A. V. Goltsev, and J. F. F. Mendes, Inverting the Achlioptas rule for explosive percolation, Phys. Rev. E **91**, 042130 (2015).

[60] M. E. J. Newman and R. M. Ziff, Fast Monte Carlo algorithm for site or bond percolation, Phys. Rev. E **64**, 016706 (2001).

[61] V. Privman and M. E. Fisher, Universal critical amplitudes in finite-size scaling, Phys. Rev. B **30**, 322 (1984).

[62] V. Privman, *Finite Size Scaling and Numerical Simulation of Statistical Systems* (World Scientific, Singapore, 1990).

[63] J.-S. Wang and R. B. Pandey, Kinetics and Jamming Coverage in a Random Sequential Adsorption of Polymer Chains, Phys. Rev. Lett. **77**, 1773 (1996).

[64] G. Kondrat and A. Pękalski, Percolation and jamming in random sequential adsorption of linear segments on a square lattice, Phys. Rev. E **63**, 051108 (2001).

[65] M. G. Slutskii, L. Y. Barash, and Y. Y. Tarasevich, Percolation and jamming of random sequential adsorption samples of large linear k-mers on a square lattice, Phys. Rev. E **98**, 062130 (2018).